

## Surface-enhanced Raman Scattering Study of the Binding Modes of a Dibenzotetraaza[14]annulene Derivative with DNA/RNA Polynucleotides<sup>†</sup>

Snežana Miljanić,<sup>a,\*</sup> Adriana Dijanošić,<sup>a</sup> Matea Kalac,<sup>a</sup> Marijana Radić Stojković,<sup>b</sup> Ivo Piantanida,<sup>b</sup> Dariusz Pawlica,<sup>c</sup> and Julita Eilmes<sup>c</sup>

<sup>a</sup>Laboratory of Analytical Chemistry, Department of Chemistry, Faculty of Science, University of Zagreb, Horvatovac 102a, HR-10000 Zagreb, Croatia

<sup>b</sup>Laboratory for Study of Interactions of Biomacromolecules, Division of Chemistry and Biochemistry, Ruđer Bošković Institute, P.O.B. 1016, HR-10000 Zagreb, Croatia

<sup>c</sup>Department of Chemistry, Jagiellonian University, Ingardena 3, 30-060 Krakow, Poland.

RECEIVED MAY 14, 2012; REVISED DECEMBER 11, 2012; ACCEPTED DECEMBER 11, 2012

**Abstract.** Binding modes of a dibenzotetraaza[14]annulene (DBTAA) derivative with synthetic nucleic acids were studied using surface-enhanced Raman spectroscopy (SERS). Changes in SERS intensity and appearance of new bands in spectra were attributed to different complexes formed between the DBTAA molecules and DNA/RNA polynucleotides. A decrease in intensity pointed to intercalation as the dominant binding mode of the annulene derivative with poly dGdC-poly dGdC and poly rA-poly rU, whereas new bands in the spectra at 735 cm<sup>-1</sup> and 1345 cm<sup>-1</sup> revealed binding within the minor groove of poly dAdT-poly dAdT. When all the dominant binding sites were occupied, SERS spectra implied that small molecules bind on the outside of the DNA analogues, while exist mainly as free molecules in equimolar ratio with the synthetic RNA polynucleotide, thereby indicating higher affinity for DNA than for RNA. (doi: 10.5562/cca2106)

**Keywords:** surface-enhanced Raman scattering, binding, polynucleotide, annulene

### INTRODUCTION

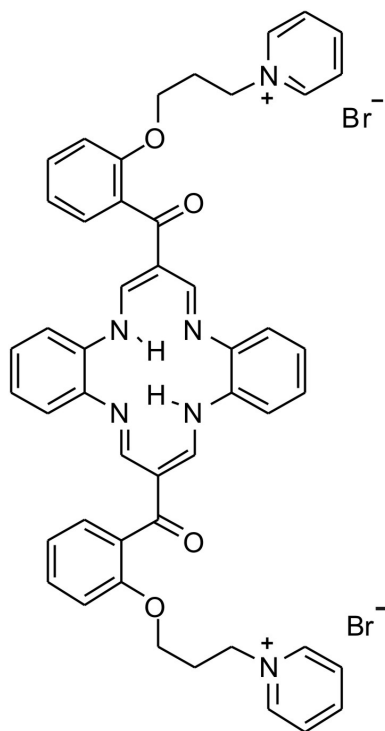
Owing to their structural resemblance to porphyrins, widely known for their diversity of interactions with DNA,<sup>1–5</sup> dibenzotetraaza[14]annulenes (DBTAA) have attracted much attention as molecules having potential nucleic acid binding ability. A series of bis-cationic DBTAA derivatives has been recently synthesized differing in pendant substituents at the *meso* positions of the planar macrocycle.<sup>6–9</sup> Side chains varied in length, rigidity and the end moiety carrying the positive charge. The syntheses were aimed at the fine tuning of the substituents structure, able to affect the DNA/RNA binding properties of the molecules. While the planar DBTAA core could intercalate between the base pairs, long and flexible linkers, incorporating polar groups could facilitate groove binding. Apart from electrostatic interactions with the anionic phosphate backbone, cationic substituents, if pyridinium based, could provide additional aromatic  $\pi$ - $\pi$  interactions with the nucleobases.

Similarly to porphyrins, which bind with DNA in three different ways: intercalation, minor/major groove

binding and outside binding with self-stacking of the DNA helix,<sup>1–5</sup> studied DBTAA derivatives showed distinctive binding modes.<sup>6–9</sup> Although all were able to interact with the nucleic acid, selectivity towards nucleic base sequences was obtained, clearly dependent on the size and structure of positively charged substituents attached to the macrocyclic moiety. Hereby, intercalation was suggested as the dominant binding mode, while the side chains were assumed to be responsible for additional binding interactions within the polynucleotide grooves. Hence, the DBTAA derivative (**DBTAAbpp**) with *meso* substituents consisting of an *o*-substituted benzoyl ring, a propoxy chain and a positively charged pyridinium group at the end, showed pronounced A–T(U) over G–C sequence preference as well as stronger thermal stabilization of DNA than RNA.<sup>9</sup> Despite extensive studies by means of UV/Vis absorption and fluorescence spectroscopy, circular dichroism, thermal denaturation and viscometry measurements, which all provided very valuable information about binding modes between small molecules and polynucleotides, accurate placement of the studied DBTAA mole-

<sup>†</sup> This article belongs to the Special Issue devoted to the 85<sup>th</sup> anniversary of *Croatica Chemica Acta*.

\* Author to whom correspondence should be addressed. (E-mail: miljanic@chem.pmf.hr)



**Scheme 1.** Chemical structure of the DBTAA derivative (DBTAAbpp).

cules with respect to the polynucleotides structure still remained unclear.<sup>8,9</sup> A use of a method revealing molecular structures of interacting species is therefore highly desirable.

Surface-enhanced Raman spectroscopy (SERS) provides structural data of the molecules adsorbed on rough metal surfaces.<sup>10</sup> Great enhancement of the Raman scattering and strong fluorescence quenching make this method suitable for vibrational studies of light emitting molecules at submicromolar concentrations. These advantages have imposed SERS as a very valuable tool for biomolecular recognition studies.<sup>11–20</sup> Related to structural changes, spectral patterns of free and bound drug molecules reveal binding sites, suggesting binding modes between small molecules and their targets.<sup>16,17,19,20</sup> Dependence of SERS spectra on the orientation of the molecules on the metal surface and surface selection rules make enhancement of the scattered radiation indicative of placement of the studied molecules relative to the metal surface. Hence band intensities differ for the free small molecules and those complexed with the nucleic acid, implying changes in position and accessibility of the molecules to the metal upon binding.<sup>11,14,15,20</sup>

Here, we report on a detailed SERS study of the binding modes of the DBTAA derivative, **DBTAAbpp**, with synthetic DNA and RNA (Scheme 1). In order to investigate influence of nucleic base sequence on the

binding, double-stranded (ds) polynucleotides (poly dAdT-poly dAdT, poly dGdC-poly dGdC and poly rA-poly rU) have been used for preparation of the complexes of various **DBTAAbpp**/ds-polynucleotide ratios. Based on analysis and interpretation of the measured SERS spectra preferential binding modes between the interacting species have been proposed.

## EXPERIMENTAL

### Chemicals and Solutions

Silver nitrate (Kemika) and trisodium citrate (Kemika) were of analytical reagent grade and used as supplied for the silver colloid preparation. Water was purified by passage through Milli-Q (Millipore) deionizing and filtration columns.

Cacodylate buffer contained sodium cacodylate (Sigma),  $c = 0.05 \text{ mol dm}^{-3}$ , adjusted to pH 7.0 by HCl (Kemika),  $c = 0.1 \text{ mol dm}^{-3}$ . Polynucleotides were purchased as noted: poly dA, poly dT, poly dAdT-poly dAdT, poly dGdC-poly dGdC and poly rA-poly rU (Sigma). Polynucleotides were dissolved in Na-cacodylate buffer,  $I = 0.05 \text{ mol dm}^{-3}$ , pH = 7.0. The concentration of double-stranded (ds) and single-stranded (ss) polynucleotides was determined spectroscopically as the concentration of phosphates.<sup>21</sup>

Detailed synthesis and spectroscopic characterization of 7,16-bis{2-[3-(*N*-pyridinium-1-yl)propoxy]benzoyl}-5,14-dihydrodibenzo[*b,i*][1,4,8,11]tetraazacyclotetradecine dibromide dihydrate (**DBTAAbpp**) has been published elsewhere.<sup>8</sup> Stock solution of **DBTAAbpp** was prepared by dissolving the substance in water of Milli-Q purity resulting in the final concentration of  $1 \times 10^{-3} \text{ mol dm}^{-3}$ .

### Colloid Preparation

Before preparation of colloid all glassware was thoroughly cleaned with a detergent solution, followed by treatment in 5 % nitric acid, and finally rinsed with water of Milli-Q purity. Silver colloid was prepared according to the modified Lee and Meisel reduction method with citrate.<sup>22,23</sup> Aqueous solution of 1 % (w/v) trisodium citrate ( $2 \text{ cm}^3$ ) was added to boiling solution of  $1 \times 10^{-3} \text{ mol dm}^{-3}$  silver nitrate ( $100 \text{ cm}^3$ ) and kept boiling for 90 minutes. The resulting colloidal solution was greenish yellow with the maximum at 421 nm in the UV/Vis absorption spectrum and the pH value of 7.7.

### Samples Preparation

For the concentration dependent SERS measurements samples were prepared by mixing the silver citrate colloid ( $400 \mu\text{L}$ ), appropriate volume of the **DBTAAbpp** stock solutions ( $1 \times 10^{-3}$  or  $1 \times 10^{-4} \text{ mol dm}^{-3}$ ) and Milli-Q water, contributing to the total volume of

500  $\mu\text{L}$ . The final concentrations of **DBTAAbpp** were  $1 \times 10^{-7}$ ,  $5 \times 10^{-7}$ ,  $1 \times 10^{-6}$ ,  $5 \times 10^{-6}$ ,  $1 \times 10^{-5}$ ,  $5 \times 10^{-5}$  and  $1 \times 10^{-4}$  mol  $\text{dm}^{-3}$ .

Interactions with the DNA/RNA polynucleotides were studied in the silver colloid containing **DBTAAbpp**,  $c = 5 \times 10^{-6}$  mol  $\text{dm}^{-3}$ , and a respective ds-polynucleotide in the  $[\text{DBTAAbpp}]/[\text{phosphate}]$  ratios of 1/1, 1/2, 1/5, 1/7 and 1/10. Samples were prepared by mixing the solution of **DBTAAbpp**,  $c = 5 \times 10^{-5}$  mol  $\text{dm}^{-3}$  (50  $\mu\text{L}$ ) with the appropriate volume of the ds-polynucleotide ( $1 \times 10^{-3}$  or  $1 \times 10^{-2}$  mol  $\text{dm}^{-3}$ ), followed by addition of the silver colloid (400  $\mu\text{L}$ ). A total volume of the working samples was 500  $\mu\text{L}$ .

Interactions with ss-polynucleotides were studied in the silver colloid containing **DBTAAbpp**,  $c = 5 \times 10^{-6}$  mol  $\text{dm}^{-3}$ , and poly dA or poly dT ( $c = 5 \times 10^{-6}$  and  $2.5 \times 10^{-5}$  mol  $\text{dm}^{-3}$ ) resulting in the mixtures of the  $[\text{DBTAAbpp}]/[\text{phosphate}]$  ratios of 1/1 and 1/5. Working samples were prepared in the same way as the mixtures of **DBTAAbpp** with ds-polynucleotides.

### Instrumentation

FT-Raman and SERS spectra were measured on a Bruker Equinox 55 interferometer equipped with a FRA 106/S Raman module using Nd-YAG laser excitation at 1064 nm and a laser power of 100 and 500 mW for measurement of the crystalline substance and colloidal samples, respectively. Raman spectrum of **DBTAAbpp** was recorded from the solid on an aluminium holder, while glass vials were used for handling SERS samples. Spectra were taken in the 3500–100  $\text{cm}^{-1}$  range. To obtain good spectral definition, 128 scans at a spectral resolution of 4  $\text{cm}^{-1}$  were averaged for a spectrum. In addition, three spectra were measured for each SERS sample which was thoroughly shaken in between measurements, and the averaged spectrum is shown in figures.

UV/Vis/NIR absorption measurements were carried out with an Analytik Jena spectrometer (model SPECORD 200). Absorption spectra were measured in the 200–1100 nm range. Conventional quartz cells (10 mm  $\times$  10 mm) were used throughout.

For pH measurements, a Mettler Toledo pH meter (model FE20 FiveEasy) with a Mettler Toledo LE409 glass electrode was used. The pH meter was calibrated with standard aqueous buffer solutions of pH 7.00 and 4.01.

## RESULTS AND DISCUSSION

### FT-Raman Spectrum of **DBTAAbpp**

The FT-Raman spectrum of crystalline **DBTAAbpp** is given in Figure 1. Medium bands in the region 3100–3000  $\text{cm}^{-1}$  are assigned to the stretchings of the

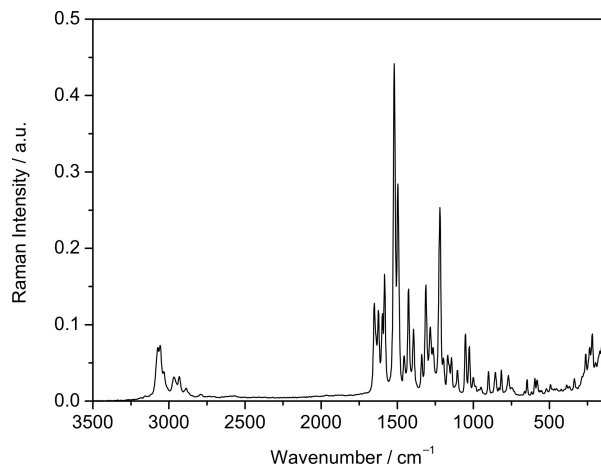


**Figure 1.** FT-Raman spectrum of **DBTAAbpp**. The spectrum was taken using 1064 nm excitation (Nd:YAG laser, 100 mW).

CH bonds in the aromatic rings. While a weak band at 2967  $\text{cm}^{-1}$  is attributed to the CH stretching of the HC=N moieties, bands at 2932 and 2887  $\text{cm}^{-1}$  are assigned to the antisymmetrical and symmetrical CH stretching of the methylene groups, respectively. The CC and CN stretching vibrations of the pyridinium, diimine and phenylene parts of the molecule give rise to the medium and strong bands in the range between 1660 and 1490  $\text{cm}^{-1}$  (Table 1).<sup>24,25</sup> Hereby, the most intense band, observed at 1520  $\text{cm}^{-1}$ , originates from the CH bendings in the central core of **DBTAAbpp**.<sup>25</sup> The CH deformation modes, mostly in diimine and phenylene, also contribute to the bands of moderate intensity at 1283, 1265, 1219, 1168 and 1144  $\text{cm}^{-1}$ . Weak bands below 1110  $\text{cm}^{-1}$  correspond mainly to the skeletal deformations of the macrocycle and pyridinium rings.<sup>24,25</sup>

### Concentration Dependence

SERS spectra of the silver citrate colloidal samples of **DBTAAbpp** were measured in the concentration range from  $1 \times 10^{-7}$  to  $1 \times 10^{-4}$  mol  $\text{dm}^{-3}$  (Figure 2). The SERS spectrum of the colloidal sample containing the lowest concentration of **DBTAAbpp**,  $1 \times 10^{-7}$  mol  $\text{dm}^{-3}$ , corresponds to the Raman spectrum of the silver citrate colloid. Increasing concentration of **DBTAAbpp** the SERS intensity increases, reaching its maximum at  $1 \times 10^{-5}$  mol  $\text{dm}^{-3}$ . With further increase in concentration, up to  $1 \times 10^{-4}$  mol  $\text{dm}^{-3}$ , enhancement of the Raman scattering weakens. Given that SERS spectra depend on the orientation of the molecules on the metal surface,<sup>10</sup> whereby vibrations with polarizability change normal to the metal surface result in strongest enhancement of the scattered radiation, and those parallel with the metal surface do not contribute to scattering, it can be assumed that at concentration of  $1 \times 10^{-5}$  mol  $\text{dm}^{-3}$  the **DBTAAbpp** molecules attain optimal perpendicular

**Table 1.** Preliminary assignment of the main vibrational bands in the FT-Raman spectrum of the crystalline substance and in the SERS spectrum of **DBTAAbpp** in the silver citrate colloid,  $c(\text{DBTAAbpp}) = 1 \times 10^{-5} \text{ mol dm}^{-3}$

Raman	SERS	Assignment
3073	3068	v CH (arom)
3058		v CH (arom)
3033		v CH (arom)
2967	2974	v CH (CH=N)
2932		$\nu_{\text{as}}$ CH (CH <sub>2</sub> )
2887		$\nu_{\text{s}}$ CH (CH <sub>2</sub> )
1651		v CC/CN (pyridinium)
	1637	v CC/CN (pyridinium, diimine)
1624		v CC/CN (diimine)
1597	1596 sh	v CC (phenylene)
1583	1585	v CC (phenylene, pyridinium)
1520	1524	$\delta$ CH (diimine, phenylene)
1496	1493	v CC (diimine)
1455	1457	$\delta$ CH (diimine)
1426	1425	$\delta$ CH <sub>2</sub> sc
1393	1395	$\delta$ CH, $\delta$ NH (diimine)
1339	1344 sh	$\delta$ CH (diimine)
1312	1318	$\delta$ CH <sub>2</sub> wg, $\delta$ CH (phenylene)
1283	1287	$\delta$ CH (diimine, phenylene, pyridinium)
1265	1267	$\delta$ CH (diimine, phenylene)
1219	1220	$\delta$ CH (diimine, phenylene)
1197	1194 sh	v C–O
1168	1167	$\delta$ CH (phenylene)
1144	1149	$\delta$ CH (diimine, phenylene)
1104	1105	$\delta$ skel (phenylene)
1052	1052	$\delta$ skel (phenylene)
1026	1029	$\delta$ skel (diimine)
1000	1003	$\delta_{\text{oop}}$ C1H, C10H (C in C=N of diimine)
901	903	$\delta$ skel (diimine, phenylene)
856	857	$\delta$ skel (diimine, phenylene)
816	814	$\delta$ skel (pyridinium)
770	766	$\delta$ skel (phenylene), $\delta_{\text{oop}}$ NH
647	648	$\delta$ skel (diimine, phenylene, pyridinium)
617	617	$\delta$ skel (diimine, phenylene, pyridinium)
595	596	$\delta$ skel (phenylene, diimine)
582	584 sh	$\delta$ skel (phenylene, diimine)
	556	$\delta$ skel (diimine)
520	521	$\delta$ skel (diimine)
493	488	$\delta_{\text{oop}}$ CH (diimine)
336		$\delta_{\text{s}}$ NCC
262		$\delta$ skel (pyridinium)
236		$\gamma_{\text{as}}$ (diimine)
	225 sh	v Ag–N
218		$\gamma_{\text{s}}$ (diimine)
	157	v Ag–Br

Abbreviations: sh, shoulder; v, stretching;  $\delta$ , deformation;  $\gamma$ , torsion; arom, aromatic; as, antisymmetrical; s, symmetrical; wg, wagging; sc, scissoring; ip, in plane; oop, out of plane; skel, skeletal.

position on the silver nanoparticles completely covering the metal surface. At concentrations lower than  $1 \times 10^{-5} \text{ mol dm}^{-3}$  weaker enhancement is attributed to a lesser

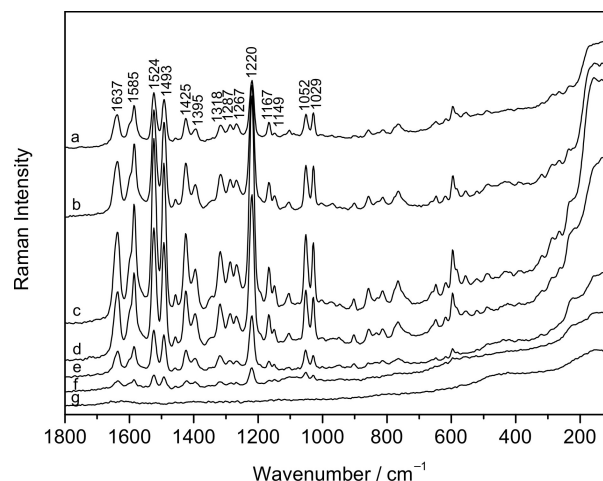


**Figure 2.** Concentration dependent SERS spectra of **DBTAAbpp**:  $1 \times 10^{-4} \text{ M}$  (a),  $5 \times 10^{-5} \text{ M}$  (b),  $1 \times 10^{-5} \text{ M}$  (c),  $5 \times 10^{-6} \text{ M}$  (d),  $1 \times 10^{-6} \text{ M}$  (e),  $5 \times 10^{-7} \text{ M}$  (f) and  $1 \times 10^{-7} \text{ M}$  (g).

number of the molecules on the nanoparticles as well as to a more space available for the molecules to place parallel with the enhancing surface. At high concentrations ( $5 \times 10^{-5}$  and  $1 \times 10^{-4} \text{ mol dm}^{-3}$ ), on the other hand, diminution in SERS intensity is a consequence of a tilted position of the molecules crowded on the silver surface. Considering the data about the crystal structure of the related DBTAA derivative, consisting of the trimethylammonium group instead of the pyridinium group in the end of the side substituents, a similar molecular structure of **DBTAAbpp** can be assumed with the benzene rings of the benzoyl group placed almost perpendicular to the planar macrocycle, directing the side chains above and below the tetraaza plane.<sup>8</sup> It is very likely that the optimal position of the molecule on the silver nanoparticles here refers to the vertical position of the macrocyclic ring near the enhancing surface.

Apart from variations in the total SERS intensity, a change in the relative intensity of the vibrational bands in the SERS spectrum additionally implies a change in position of the molecules with respect to the metal surface. If changes in band intensities were induced only by changes in concentration, intensity ratio of any two vibrational bands in the spectrum would yield a constant value regardless of concentration. To study that, ratios of the intensities of the strongest band in the spectrum ( $1220 \text{ cm}^{-1}$ ), assigned to the CH bending mode in the diimine and phenylene moieties, and the selected intense bands are calculated for **DBTAAbpp** at various concentrations (Table 2). A slight descending tendency with the concentration increase is observed for the intensity ratios of the band at  $1524 \text{ cm}^{-1}$ , attributed also to the diimine and phenylene CH deformations. Unlike the close values obtained for the band assigned to the same type of vibrations as the chosen reference

**Table 2.** Intensity ratios of the selected vibrational bands in the concentration dependent SERS spectra of **DBTAAbpp**

$c(\mathbf{1}) / \text{mol dm}^{-3}$	$I_{1220}/I_{1637}$	$I_{1220}/I_{1524}$	$I_{1220}/I_{1052}$	$I_{1220}/I_{1029}$
$1 \times 10^{-4}$	1.71	1.18	1.70	1.65
$5 \times 10^{-5}$	2.06	1.20	2.18	2.20
$1 \times 10^{-5}$	2.21	1.21	2.26	2.44
$5 \times 10^{-6}$	2.08	1.22	2.04	2.20
$1 \times 10^{-6}$	1.93	1.24	1.87	2.17
$5 \times 10^{-7}$	1.60	1.27	1.15	1.27

band, ratios concerning intensities of the bands at 1637, 1052 and 1029  $\text{cm}^{-1}$ , attributed to the pyridinium stretching and skeletal deformation modes of phenylene and diimine, respectively, significantly differ. By increasing concentration of **DBTAAbpp**, the ratio values increase up to the values evaluated for the sample of  $1 \times 10^{-5} \text{ mol dm}^{-3}$ , after which they decrease. Relative changes in band intensities suggest differently enhanced vibrational modes as a result of the concentration induced change in position of the studied molecules on the silver surface.

Furthermore, increase in concentration did not affect position of the bands in the SERS spectra, implying that the molecules of DBTAA derivative do not aggregate in the studied concentration range.<sup>15</sup> However, if compared to the Raman spectrum of the crystalline substance, instead of the medium bands at 1651 and 1624  $\text{cm}^{-1}$ , assigned to the CC/CN stretching modes of pyridinium and diimine, respectively, only one band appears at 1637  $\text{cm}^{-1}$  in the SERS spectra of **DBTAAbpp** (Table 1). In addition, in the SERS spectra a very strong band is obtained at 157  $\text{cm}^{-1}$  with a shoulder at 225  $\text{cm}^{-1}$ . The intense band is assigned to the Ag–Br stretching mode of a bond formed between the silver surface and the bromide counterions,<sup>26</sup> whereas the shoulder is attributed to the stretching of the Ag–N bond of the molecules chemisorbed on the silver nanoparticles.<sup>26,27</sup> The latter causes the charge redistribution in the nitrogen consisting moieties, responsible for the observed band shifts.<sup>28,29</sup> Apart from chemisorption, electrostatic interactions between the positive charge in the side substituents and the negatively charged citrate ions on the silver surface enable placement of the **DBTAAbpp** molecules in close vicinity to the metal nanoparticles.

#### *Interactions of DBTAAbpp with DNA and RNA Polynucleotides*

Binding of **DBTAAbpp** with the DNA and RNA analogues characterized by  $\beta$ -helical secondary structure was studied using polymers of complementary bases, poly dGdC-poly dGdC, poly dAdT-poly dAdT and poly rA-poly rU. Samples were prepared by previous mixing of **DBTAAbpp** with the polynucleotide, followed by addition of the silver citrate colloid into the mixture. Since the results of the UV/Vis absorption spectroscopy

and CD measurements pointed toward saturation of the dominant binding sites at a molar ratio of about 0.25,<sup>9</sup> the **DBTAAbpp**/ds-polynucleotide mixtures were prepared in molar ratios of 1/1, 1/2, 1/5, 1/7 and 1/10, including complexes with completely and partially occupied dominant binding sites. Concentration of **DBTAAbpp** was  $5 \times 10^{-6} \text{ mol dm}^{-3}$  and kept constant in all working samples. SERS spectra of the polynucleotides alone were not observed. Repulsive forces between the negatively charged citrate ions on the silver nanoparticles and the highly negatively charged phosphate backbone of the polynucleotides prevented adsorption of the molecules on the enhancing silver surface.<sup>30,31</sup>

*Interactions of DBTAAbpp with poly dGdC-poly dGdC*  
SERS spectra of the **DBTAAbpp**/poly dGdC-poly dGdC complexes are given in Figure 3. In comparison with the SERS spectrum obtained for free **DBTAAbpp** molecules, weaker enhancement for DBTAA derivative molecules is observed in the presence of the polynucleotide at all measuring ratios,  $r_{[\text{DBTAAbpp}]/[\text{poly dGdC-poly dGdC}]}$ . Since the samples with and without poly dGdC-poly dGdC contained the same concentration of small molecules ( $5 \times 10^{-6} \text{ mol dm}^{-3}$ ), poor scattering from the

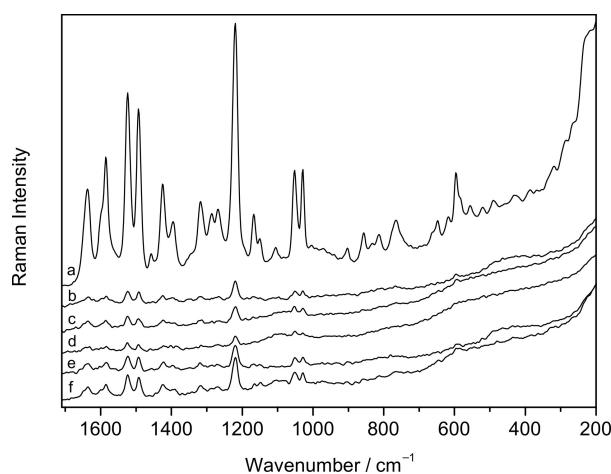


**Figure 3.** SERS spectra of **DBTAAbpp** (a) and the **DBTAAbpp**/poly dGdC-poly dGdC complexes at the molar ratios of 1/1 (b), 1/2 (c), 1/5 (d), 1/7 (e) and 1/10 (f);  $c(\text{DBTAAbpp}) = 5 \times 10^{-6} \text{ M}$ .

complexes is a consequence of either a tilted position of the molecules towards the enhancing surface or a hindered approach of the molecules to the silver surface, both induced by interactions with the polynucleotide. In the **DBTAAbpp**/poly dGdC-poly dGdC mixtures of the 1/1 and 1/2 ratios, when all the dominant binding sites are taken, small molecules are able to bind externally to the polynucleotide.<sup>5</sup> Bound on the outside of the polynucleotide helical structure, the DBTAA derivative molecules are not capable of taking the optimal perpendicular position on the metal surface, resulting in the surface scattering decrease. On the other hand, the SERS spectra of the samples containing the excess of polynucleotide binding sites over the studied compound (**DBTAAbpp**/poly dGdC-poly dGdC 1/5, 1/7 and 1/10) correspond to the favored binding mode of **DBTAAbpp** with the guanine-cytosine polynucleotide. Low SERS intensity here implies intercalation of the small molecules within the poly dGdC-poly dGdC helix.<sup>11,14,15</sup> Due to a deep insertion of the planar DBTAA core of **DBTAAbpp** between the base pairs the molecules are placed away from the silver surface, resulting in a weaker enhancement of the scattered radiation.

#### *Interactions of DBTAAbpp with poly dAdT-poly dAdT*

Unlike a lack of a clear difference between the SERS spectra corresponding to the complexes of **DBTAAbpp** with poly dGdC-poly dGdC having occupied and unoccupied dominant binding sites, different SERS spectra were obtained for the **DBTAAbpp**/poly dAdT-poly dAdT mixtures (Figure 4). Hence spectra of the 1/1 and 1/2 complexes are characterized by weak scattering enhancement, most likely for the same reason as for the respective mixtures of **DBTAAbpp** with the guanine-cytosine polynucleotide. Filling the dominant binding sites in poly dAdT-poly dAdT, the small molecules tend to bind on the outside of the polynucleotide resulting in an inclined position close to the silver surface. Increasing the content of the adenine-thymine polynucleotide in the mixture, the SERS intensity increases. The spectra of the **DBTAAbpp**/poly dAdT-poly dAdT complexes of 1/5, 1/7 and 1/10 imply binding, clearly different from that with poly dGdC-poly dGdC. Although the results of previously used spectroscopic methods point to intercalation as the binding mode of **DBTAAbpp** with poly dAdT-poly dAdT,<sup>9</sup> stronger SERS intensity implies a position of the complexed **DBTAAbpp** molecules closer to the enhancing surface than that in the complex with poly dGdC-poly dGdC. It can be assumed that due to additional interactions, such as those within the polynucleotide grooves, the planar macrocycle of the DBTAA derivative is drawn from the polynucleotide helix, not being completely inserted between the base pairs.

Although shifts of the vibrational bands in the SERS spectra of the free and bound molecules are not

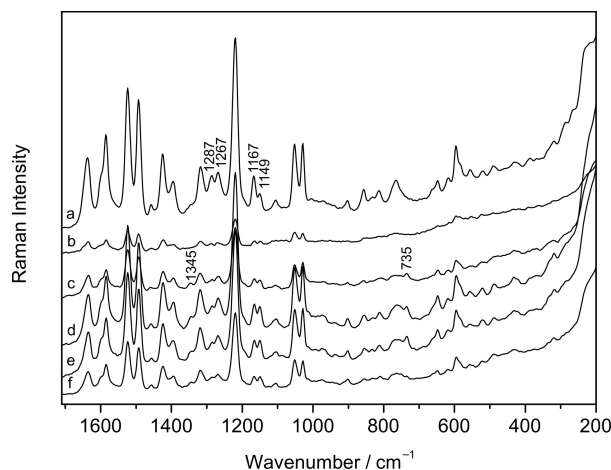


**Figure 4.** SERS spectra of **DBTAAbpp** (a) and the **DBTAAbpp**/poly dAdT-poly dAdT complexes at the molar ratios of 1/1 (b), 1/2 (c), 1/5 (d), 1/7 (e) and 1/10 (f);  $c(\text{DBTAAbpp}) = 5 \times 10^{-6}$  M.

observed, relative changes in band intensities are obtained. For instance, the intensity ratio of the bands at 1167 and 1149  $\text{cm}^{-1}$ , attributed to the CH bending in phenylene and diimine, is 1.29 in the spectrum of the free molecules, while in the spectrum of the **DBTAAbpp**/poly dAdT-poly dAdT 1/5 mixture it decreases to a value of 1.03. Another example is a change in the intensity concerning bands at 1287 and 1267  $\text{cm}^{-1}$ , assigned to the CH deformation modes in the diimine, phenylene and pyridinium groups, for which the intensity ratio is 0.96 in the spectrum of **DBTAAbpp** alone, and 0.89 in the spectrum of the 1/5 complex. Relative changes in band intensities imply that upon binding with the adenine-thymine polynucleotide the DBTAA derivative molecules adopt different positions on the silver surface.

Moreover, in the SERS spectra of **DBTAAbpp**/poly dAdT-poly dAdT two new bands were obtained. One band is observed at 735  $\text{cm}^{-1}$  and preliminary assigned to the ring breathing modes of the nucleic bases, adenine and/or thymine. According to Nakamoto *et al.* the corresponding Raman bands for adenine and thymine appear at 724 and 741  $\text{cm}^{-1}$ , respectively.<sup>32</sup> Another new band is noted at 1345  $\text{cm}^{-1}$  and could be due to either vibration of the adenine<sup>32</sup> or enhancement of the vibrational mode of **DBTAAbpp**, which primarily appears as a shoulder at 1344  $\text{cm}^{-1}$ . In order to study the origin of the new bands appearing in the SERS spectra, mixtures of **DBTAAbpp** with the single-stranded polynucleotides, poly dA and poly dT, in ratios of 1/1 and 1/5 were prepared. Whereas the SERS spectra of the 1/1 mixtures are weaker in intensity but resemble the spectrum of the free small molecules, very weak spectra of the 1/5 mixtures did not allow analysis of the vibrational bands of inter-

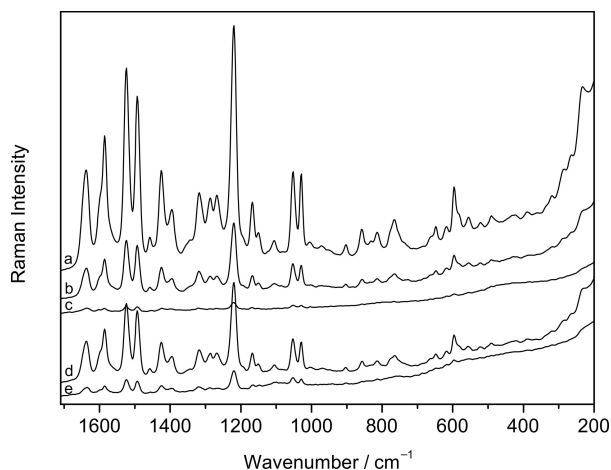


**Figure 5.** SERS spectra of **DBTAAbpp** (a), **DBTAAbpp**/poly dA 1/1 (b), **DBTAAbpp**/poly dA 1/5 (c), **DBTAAbpp**/poly dT 1/1 (d) and **DBTAAbpp**/poly dT 1/5 (e);  $c(\text{DBTAAbpp}) = 5 \times 10^{-6}$  M.

est (Figure 5). It is very likely that long flexible single stranded polynucleotides twine around the molecule preventing it to come close to the enhancing silver surface.

Regarding the fact that there is no band close to  $735 \text{ cm}^{-1}$  neither in the Raman spectrum nor in the SERS spectrum of **DBTAAbpp**, the new band is attributed to the poly dAdT-poly dAdT polynucleotide, i.e. vibrational modes of thymine and/or the six-membered ring of adenine. The C=O group of thymine and N3 atom of adenine are not involved in the Watson-Crick pairing and therefore are available for interactions with the molecules in the minor groove of the polynucleotide. On the contrary, the guanine amino group of the poly dGdC-poly dGdC polynucleotide introduces a sterical hindrance in the minor groove, making it a less favourable binding site for small molecules.<sup>33,34</sup> The band at  $1345 \text{ cm}^{-1}$ , however, could not be unambiguously assigned, except for the fact that appeared in the spectrum upon binding with the polynucleotide. Therefore it is reasonable to assume, that beside intercalation the **DBTAAbpp** molecules bind within the minor groove of poly dAdT-poly dAdT, too.

#### Interactions of **DBTAAbpp** with poly rA-poly rU

The SERS spectra of the **DBTAAbpp**/poly rA-poly rU complexes are given in Figure 6. In contrast to the spectra of the complexes with the DNA polynucleotides, the most intense spectrum is obtained for the mixture of **DBTAAbpp** with the RNA analogue containing the same concentration of the interacting species. Considering band positions and relative band intensities the spectrum of the **DBTAAbpp**/poly rA-poly rU 1/1 mixture is very similar to the SERS spectrum of **DBTAAbpp**, indicating that the free molecules of the DBTAA de-

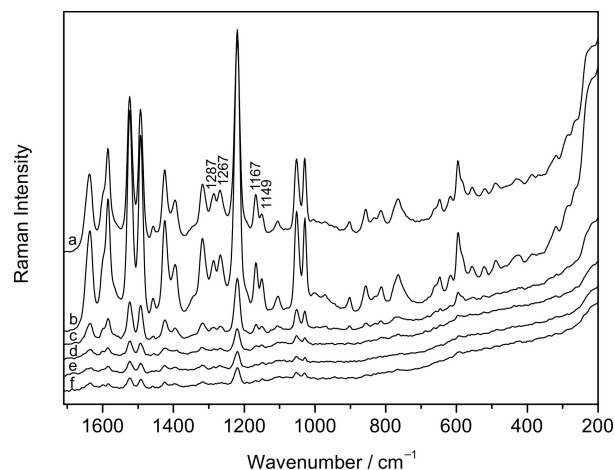


**Figure 6.** SERS spectra of **DBTAAbpp** (a) and the **DBTAAbpp**/poly rA-poly rU complexes at the molar ratios of 1/1 (b), 1/2 (c), 1/5 (d), 1/7 (e) and 1/10 (f);  $c(\text{DBTAAbpp}) = 5 \times 10^{-6}$  M.

riivative on the silver surface contribute at most to the measured spectrum. The obtained difference between the SERS spectra of the annulene molecules in the equimolar ratios with the DNA analogues and the synthetic RNA implies higher affinity of the DBTAA derivative for DNA than for RNA. Increasing the content of the RNA polynucleotide in the mixture, SERS intensity decreases and does not change significantly for the mixtures of the 1/5, 1/7 and 1/10 ratios. Weak enhancement of the surface scattering obtained from the complexes with the excess of the polynucleotide binding sites points to intercalation as the dominant binding mode.<sup>11,15</sup> It is interesting to note that in the spectrum of the **DBTAAbpp**/poly rA-poly rU 1/5 complex the intensity ratio of the bands at  $1287$  and  $1267 \text{ cm}^{-1}$ , attributed to the vibrational modes of pyridinium, diimine and phenylene, is 0.95 and is very similar to the value calculated for the free molecules (0.96), at variance to the value of 0.89 characteristic of the **DBTAAbpp**/poly dAdT-poly dAdT 1/5 complex. Since minor groove binding is proposed as the binding mode with the adenine-thymine polynucleotide and not obtained with the RNA polynucleotide, the calculated ratio could be indicative of interactions of the DBTAA derivative within the minor groove. Despite resemblance in molecular structures of the A-T and A-U nucleic bases, a wide and shallow minor groove of the adenine-uracil polynucleotide prevents efficient binding of the small molecules.<sup>34</sup>

## CONCLUSION

Surface selection rules of the SERS spectroscopy allowed interpretation of the scattering enhancement ob-

tained from the DBTAA derivative bound with the DNA and RNA polynucleotides. Changes in SERS intensity induced by interactions with the polynucleotides were attributed to different complexes formed depending on the availability of the polynucleotide binding sites. Hence, intercalation was revealed as the dominant binding mode of **DBTAAbpp** with poly dGdC-poly dGdC and poly rA-poly rU, whereas binding within the minor groove of poly dAdT-poly dAdT was also considered. When all the dominant binding sites were occupied, SERS spectra indicated that the **DBTAAbpp** molecules bind on the outside of the DNA analogues, while exist mainly as free molecules in equimolar ratio with the synthetic RNA. Providing structural data about interacting species, SERS showed its potential as a technique used along with other spectroscopic methods for obtaining a consistent picture of the binding modes.

*Acknowledgements.* This research was supported by the Croatian Ministry of Science, Education and Sports (project nos. 119-1191342-2959 and 098-0982914-2918).

## REFERENCES

1. R. J. Fiel, *J. Biomol. Struct. Dyn.* **6** (1989) 1259–1274.
2. L. G. Marzilli, *New J. Chem.* **14** (1990) 409–420.
3. R. F. Pasternack and E. J. Gibbs, *Met. Ions Biol. Syst.* **33** (1996) 367–397.
4. U. Sehlstedt, S. K. Kim, P. Carter, J. Goodisman, J. F. Vollano, B. Nordén, and J. C. Dabrowiak, *Biochemistry* **33** (1994) 417–426.
5. X. Chen and M. Liu, *J. Inorg. Biochem.* **94** (2003) 106–113.
6. D. Pawlica, M. Radić Stojković, L. Sieroń, I. Piantanida, and J. Eilmes, *Tetrahedron* **62** (2006) 9156–9165.
7. M. Radić Stojković, I. Piantanida, M. Kralj, M. Marjanović, M. Žinić, D. Pawlica, and J. Eilmes, *Bioorg. Med. Chem.* **15** (2007) 1795–1801.
8. D. Pawlica, M. Radić Stojković, Ł. Dudek, I. Piantanida, L. Sieroń, and J. Eilmes, *Tetrahedron* **65** (2009) 3980–3989.
9. M. Radić Stojković, M. Marjanović, D. Pawlica, L. Dudek, J. Eilmes, M. Kralj, and I. Piantanida, *New J. Chem.* **34** (2010) 500–507.
10. R. Aroca, *Surface-enhanced Vibrational Spectroscopy*, John Wiley & Sons, West Sussex, 2006, pp. 73–106.
11. G. Breuzard, J.-M. Millot, J.-F. Riou, and M. Manfait, *Anal. Chem.* **75** (2003) 4305–4311.
12. A. Murza, S. Alvarez-Méndez, S. Sanchez-Cortes, and J. V. Garcia-Ramos, *Biopolymers* **72** (2003) 174–184.
13. W. Xie, Y. Ye, A. Shen, L. Zhou, Z. Lou, X. Wang, and J. Hu, *Vib. Spectrosc.* **47** (2008) 119–123.
14. P. Zhao, L.-C. Xu, J.-W. Huang, B. Fu, H.-C. Yu, W.-H. Zhang, J. Chen, J.-H. Yao, and L.-N. Ji, *Bioorg. Chem.* **36** (2008) 278–287.
15. S. Miljanić, A. Dijanošić, I. Matošević, and I. Piantanida, *Vib. Spectrosc.* **57** (2011) 23–29.
16. A. Ianoul, F. Fleury, O. Duval, R. Waigh, J.-C. Jardillier, A. J. P. Alix, and I. Nabiev, *J. Phys. Chem. B* **103** (1999) 2008–2013.
17. M. Ermishov, A. Sukhanova, E. Kryukov, S. Grokhovsky, A. Zhuze, V. Oleinikov, J.-C. Jardillier, and I. Nabiev, *Biopolymers* **57** (2000) 272–281.
18. C.-Y. Wu, W.-Y. Lo, C.-R. Chiu, and T.-S. Yang, *J. Raman Spectrosc.* **37** (2006) 799–807.
19. S. Miljanić, A. Dijanošić, I. Piantanida, Z. Meić, M. Teresa Albelda, A. Sornosa-Ten, and E. García-España, *Analyst* **136** (2011) 3185–3193.
20. S. Miljanić, A. Dijanošić, K. Landeka, M. Radić Stojković, and I. Piantanida, *Appl. Spectrosc.* **66** (2012) 82–89.
21. B. S. Palm, I. Piantanida, M. Žinić, and H.-J. Schneider, *J. Chem. Soc. Perkin Trans. 2* (2000) 385–392.
22. P. C. Lee and D. Meisel, *J. Phys. Chem. B* **86** (1982) 3391–3395.
23. C. H. Munro, W. E. Smith, M. Garner, J. Clarkson, and P. C. White, *Langmuir* **11** (1995) 3712–3720.
24. F. R. Dollish, W. G. Fateley, and F. F. Bentley, *Characteristic Raman Frequencies of Organic Compounds*, John Wiley & Sons, New York, 1974.
25. S. Gawinkowski, J. Eilmes, and J. Waluk, *J. Mol. Struct.* **976** (2010) 215–225.
26. E. J. Liang, C. Engert, and W. Kiefer, *Vib. Spectrosc.* **8** (1995) 435–444.
27. G. Cardini, M. Muniz-Miranda, M. Pagliai, and V. Schettino, *Theor. Chem. Acc.* **117** (2007) 451–458.
28. A. Vivoni, R. L. Birke, R. Foucault, and J. R. Lombardi, *J. Phys. Chem. B* **107** (2003) 5547–5557.
29. L. Zhao, L. Jensen, and G. C. Schatz, *J. Am. Chem. Soc.* **128** (2006) 2911–2919.
30. W. Ke, D. Zhou, J. Wu, and K. Ji, *Appl. Spectrosc.* **59** (2005) 418–423.
31. K. Faulds, W. E. Smith, and D. Graham, *Analyst* **130** (2005) 1125–1131.
32. K. Nakamoto, M. Tsuboi, and G. D. Strahan, *Drug-DNA Interactions: Structures and Spectra*, John Wiley & Sons, New Jersey, 2008.
33. A. D. Neto and A. A. M. Lapis, *Molecules* **14** (2009) 1725–1745.
34. S. Neidle, *Principles of Nucleic Acid Structure*, Elsevier, London, 2008.